Conservative Power Theory, a Framework to Approach Control and Accountability Issues in Smart Microgrids

Paolo Tenti, *Fellow, IEEE*, Helmo Kelis Morales Paredes, *Student Member, IEEE*, and Paolo Mattavelli, *Member, IEEE*

***Abstract*—Smart microgrids offer a new challenging domain for power theories and compensation techniques, because they include a variety of intermittent power sources, which can have dynamic impact on power flow, voltage regulation, and distribution losses. When operating in the islanded mode, low-voltage smart microgrids can also exhibit considerable variation of amplitude and frequency of the voltage supplied to the loads, thus affecting power quality and network stability. Due to limited power capability in smart microgrids, the voltage distortion can also get worse, affecting measurement accuracy, and possibly causing tripping of protections. In such context, a reconsideration of power theories is required, since they form the basis for supply and load characterization, and accountability. A revision of control techniques for harmonic and reactive compensators is also required, because they operate in a strongly interconnected environment and must perform cooperatively to face system dynamics, ensure power quality, and limit distribution losses. This paper shows that the conservative power theory provides a suitable background to cope with smart microgrids characterization needs, and a platform for the development of cooperative control techniques for distributed switching power processors and static reactive compensators.**

***Index Terms*—Conservative power theory (CPT), distributed control, electronic power processors, power measurement, revenue metering, smart microgrids.**

I. Introduction

SMART grids represent one of the grand challenges at planetary level. The infusion of information technology throughout the electric grid creates new capabilities, with potential impact on environment, science and technology, economics, and lifestyle. The term "smart grid" outlines the evolution of electrical grids and a change of paradigm in the electric market organization and management [30], [31]. In a global perspective, implementation of smart grids and microgrids on a large scale will result in dramatic improvement of electrical services and considerable market increase.

Manuscript received June 30, 2010; revised October 8, 2010; accepted November 8, 2010. Date of current version May 13, 2011. Recommended for publication by Associate Editor R. Burgos.

P. Tenti is with the Department of Information Engineering, University of Padova, Padova 35131, Italy (e-mail: tenti@dei.unipd.it).

H. K. Morales Paredes is with the Department of Electrical Energy Systems, University of Campinas, Campinas, São Paulo 13083-852, Brazil (e-mail: hmorales@dsee.fee.unicamp.br).

P. Mattavelli is with the Center of Power Electronics Systems (CPES), Virginia Polytechnic Institute and State University, Blacksburg, VA 24061 USA (e-mail: pmatta@vt.edu).

Color versions of one or more of the figures in this paper are available online at http://ieeexplore.ieee.org.

Digital Object Identifier 10.1109/TPEL.2010.2093153

Technically speaking, smart grids include a number of distributed energy resources and electronic power processors, which must be fully exploited to reduce carbon footprint, improve power quality, and increase distribution efficiency [22], [32], [34]. The *smart-grid paradigm* is therefore different from the traditional one, based on the assumption of few power sources with large capacity and sinusoidal supply. Especially in smart microgrids (low-voltage smart grids with installed power not exceeding the megawatt range), energy sources can be small, distributed and interacting, and supply voltages can be asymmetrical and distorted.

From the earlier considerations, it follows that facing the problems of smart grids, and in particular of smart microgrids, requires a revision of traditional power theories and a comprehensive approach to cooperative operation of distributed electronic power processors. This paper shows that the conservative power theory (CPT) offers a consistent framework to approach smart microgrid characterization and control problems. In particular, the influence of frequency variation and voltage distortion can be taken into account, and the load and supply responsibility for reactive power, asymmetry, and distortion can be analyzed, thus setting the basis for a revision for metering and billing procedures.

II. Conservative Power Terms Under Periodic Nonsinusoidal Operation

The problem of defining power and current terms under nonsinusoidal conditions dates back to some 80 years [1]. While definition of active power and current terms was developed in early 30s [2], definition of power and current terms related to "reactive" and "harmonic" phenomena is still under discussion and different solutions have been proposed depending on the field of application [2]–[12]. The CPT, presented in [5], [25], provides a background to approach the problem. The theory is summarized hereafter by making reference to the definitions given in Appendix.

Consider a polyphase network and let $\underline{u}$ and $\underline{i}$ be the vectors of phase voltages and currents measured at a generic network port, and $\underline{\widehat{u}}$ is the vector of unbiased voltage integrals [definition (A1d)]. We define the following *conservative quantities* (Appendix, Section II):

$$\text{instantaneous power} \quad p = \underline{u} \circ \underline{i} \tag{1a}$$

$$\text{instantaneous reactive energy} \quad w = \underline{\widehat{u}} \circ \underline{i}. \tag{1b}$$

The corresponding average values are as follows:

$$\text{active power} \quad P = \bar{p} = \langle \underline{u}, \underline{i} \rangle \tag{2a}$$

$$\text{reactive energy} \quad W = \bar{w} = \langle \underline{\hat{u}}, \underline{i} \rangle. \tag{2b}$$

It is worth noting that definitions (1b) and (2) hold irrespective of voltage and current waveforms, provided that they are periodic. Moreover, computation of the quantities defined by (1) and (2) is directly done in the time domain and requires integration and low-pass filtering only. Finally, since the conservation property holds in general, active power and reactive energy are additive quantities in every electrical network.

Application of (2) to basic passive network elements, considering properties (A3a) and (A3b), gives

$$\text{resistor } R: \quad u_R = R i_R \quad P_R = \frac{U_R^2}{R} \qquad W_R = 0 \tag{3a}$$

$$\text{inductor } L: \quad u_L = L \breve{i}_L \quad P_L = 0 \qquad W_L = L I_L^2 = \frac{1}{2}\bar{\varepsilon}_L \tag{3b}$$

$$\text{capacitor } C: \quad i_C = C \breve{u}_C \quad P_C = 0$$

$$W_C = -C U_C^2 = -\frac{1}{2}\bar{\varepsilon}_C. \tag{3c}$$

Thus, irrespective of voltage and current waveforms, resistors absorb only active power, while inductors and capacitors take a reactive energy, which is proportional to their average stored energy $\bar{\varepsilon}_L$ and $\bar{\varepsilon}_C$, respectively. Due to conservation property, in passive networks the total active power absorption is obtained by adding the power consumption of each resistor, while total reactive energy is computed as total average inductive energy minus total average capacitive energy.

Another relevant, though not conservative, power term characterizing the network operation at a given port is the apparent power *A*, defined by

$$A = \boldsymbol{U}\boldsymbol{I} \tag{4a}$$

where $\boldsymbol{U}$ and $\boldsymbol{I}$ are the collective rms values of phase voltages and currents, according to definition (A2c). Correspondingly, the power factor λ is defined as follows:

$$\lambda = \frac{|P|}{A}. \tag{4b}$$

In polyphase networks, the power and energy terms defined by (1) and (2) do not depend on the voltage reference, whereas apparent power and power factor depend on this choice. Irrespective of neutral wire, we adopt a voltage reference, which provides unity power factor when the load is purely resistive and symmetrical. This removes any ambiguity in the apparent power definition and allows use of the power factor as an index of power quality. To comply with this condition, in four-wire systems, the neutral voltage u_0 must be taken as reference ($u_0 = 0$), while in three-wire systems the voltage reference is set at the center point of the phase voltages. Correspondingly, the collective rms values $\boldsymbol{U}$ and $\boldsymbol{I}$ of phase voltages and currents are expressed—irrespective of neutral wire—by

$$\boldsymbol{U} = \sqrt{\langle \underline{u}, \underline{u} \rangle} = \sqrt{\sum_{n=1}^{N} U_n^2} \qquad \boldsymbol{I} = \sqrt{\langle \underline{i}, \underline{i} \rangle} = \sqrt{\sum_{n=1}^{N} I_n^2}. \tag{5}$$

Note that, in (5), only phase currents are considered, while neutral current (i_0) does not contribute to the summation. This does not mean that neutral current is disregarded, inasmuch rms phase currents are affected by homopolar terms, which reflect its presence. Note also that, with the proposed selection of voltage reference, the neutral current is not even affecting active power and reactive energy.

III. Current Terms Under Periodic Nonsinusoidal Operation

A. Basic Current Terms

Consider a generic port of a *N*-phase network and let u_n and i_n be the voltage and current measured at phase *n* terminals. We decompose current i_n so as to identify the terms related to active power P_n and reactive energy W_n absorbed by phase *n* at the given port.

1) The *active current* is the minimum phase current (i.e., with minimum rms value) needed to convey active power P_n. It is expressed by

$$i_{an} = \frac{\langle u_n, i_n \rangle}{\|u_n\|^2} u_n = \frac{P_n}{U_n^2} u_n = G_n u_n, n = 1, 2, \ldots, N$$

$$\Rightarrow \boldsymbol{I}_a = \sqrt{\sum_{n=1}^{N} I_{an}^2} = \sqrt{\sum_{n=1}^{N} \left(\frac{P_n}{U_n}\right)^2}. \tag{6}$$

In (6), term $G_n = P_n / U_n^2$ is the *equivalent conductance* of phase *n*. The active current has no impact on reactive energy, as it can easily be shown from (6) and (A.3a).

2) The *reactive current* is the minimum phase current needed to convey reactive energy W_n. It is expressed by

$$i_{rn} = \frac{\langle \hat{u}_n, i_n \rangle}{\| \hat{u}_n \|^2} \hat{u}_n = \frac{W_n}{\hat{U}_n^2} \hat{u}_n = B_n \hat{u}_n, n = 1, 2, \ldots, N$$

$$\Rightarrow \boldsymbol{I}_r = \sqrt{\sum_{n=1}^{N} I_{rn}^2} = \sqrt{\sum_{n=1}^{N} \left(\frac{W_n}{\hat{U}_n}\right)^2} \tag{7}$$

In (7), term $B_n = W_n / \hat{U}_n^2$ is the *equivalent reactivity* of phase *n*. The reactive current has no impact on active power, as it can easily be shown from (7) and (A3a.)

3) The remaining current term is called *void current* and is not conveying active power and reactive energy. It is defined by

$$i_{vn} = i_n - i_{an} - i_{rn} \; n = 1, 2, \ldots, N. \tag{8}$$

4) *Orthogonality*: All the aforementioned current terms are orthogonal, thus

$$I_n = \sqrt{I_{an}^2 + I_{rn}^2 + I_{vn}^2} \Rightarrow \boldsymbol{I} = \sqrt{\boldsymbol{I}_a^2 + \boldsymbol{I}_r^2 + \boldsymbol{I}_v^2}. \tag{9}$$

B. Balanced Current Terms

As for conventional networks under sinusoidal operation, it makes sense to identify the effects of supply voltage asymmetry and load unbalance, because they both affect power quality. Of course, under nonsinusoidal operation, the traditional approach must be revised and this can easily be done based on the earlier definitions. Notice, first of all, that we use term "unbalance" to characterize the load attitude to perform asymmetrically in the different phases. Instead, term "asymmetry" is associated to an asymmetrical behavior of the supply seen from load terminals.

Irrespective of supply asymmetry, load unbalance, and waveform distortion, we define the following current terms.

1) The *balanced active currents* are the minimum currents (i.e., with minimum collective rms value) needed to convey total active power *P* absorbed at the port. They are given by

$$\underline{i}_a^b = \frac{\langle \underline{u}, \underline{i} \rangle}{\|\underline{u}\|^2}\underline{u} = \frac{P}{\boldsymbol{U}^2}\underline{u} = G^b \underline{u} \Rightarrow \boldsymbol{I}_a^b = \frac{P}{\boldsymbol{U}}. \tag{10}$$

In (10), coefficient $G^b = P/\boldsymbol{U}^2$ is the *equivalent balanced conductance*. Note that these currents are the same that would be absorbed by a symmetrical resistive load with same active power consumption as the actual load.

2) Similarly, the *balanced reactive currents* are the currents with minimum collective rms value needed to convey total reactive energy *W* absorbed at the port. They are given by

$$\underline{i}_r^b = \frac{\langle \underline{\widehat{u}}, \underline{i} \rangle}{\|\underline{\widehat{u}}\|^2}\underline{\widehat{u}} = \frac{W}{\widehat{\boldsymbol{U}}^2}\underline{\widehat{u}} = B^b \underline{\widehat{u}} \Rightarrow \boldsymbol{I}_r^b = \frac{W}{\widehat{\boldsymbol{U}}}. \tag{11}$$

In (11), coefficient $B^b = W/\widehat{\boldsymbol{U}}^2$ is the *equivalent balanced reactivity*. Note that these currents are the same that would be absorbed by a symmetrical reactive load taking same reactive energy as the actual load.

C. Unbalanced Current Terms

1) *Unbalanced active currents* are defined by difference

$$i_{an}^u = \left(G_n - G^b\right) u_n, n = 1, 2, \ldots, N$$
$$\Rightarrow \boldsymbol{I}_a^u = \sqrt{\sum_{n=1}^{N}\left(\frac{P_n}{U_n}\right)^2 - \left(\frac{P}{\boldsymbol{U}}\right)^2}. \tag{12a}$$

Clearly, these currents exist only if the load is unbalanced, i.e., if the equivalent phase conductances differ from each other. Note that the balanced and unbalanced active currents are collectively orthogonal, i.e.,

$$\langle \underline{i}_a^u, \underline{i}_a^b \rangle = 0 \Rightarrow \boldsymbol{I}_a^u = \sqrt{\boldsymbol{I}_a^2 - \boldsymbol{I}_a^{b^2}}. \tag{12b}$$

2) Similarly, the *unbalanced reactive currents* are defined by

$$i_{rn}^u = \left(B_n - B^b\right) \widehat{u}_n, n = 1, 2, \ldots, N$$
$$\Rightarrow \boldsymbol{I}_r^u = \sqrt{\sum_{n=1}^{N}\left(\frac{W_n}{\widehat{U}_n}\right)^2 - \left(\frac{W}{\widehat{\boldsymbol{U}}}\right)^2}. \tag{13a}$$

These currents exist only if the equivalent phase reactivities differ from each other. The balanced and unbalanced reactive currents are collectively orthogonal, thus,

$$\langle \underline{i}_r^u, \underline{i}_r^b \rangle = 0 \Rightarrow \boldsymbol{I}_r^u = \sqrt{\boldsymbol{I}_r^2 - \boldsymbol{I}_r^{b^2}} \tag{13b}$$

We collectively refer to *unbalance currents* as the sum of active and reactive unbalance terms, which are orthogonal each other. Thus,

$$\underline{i}^u = \underline{i}_a^u + \underline{i}_r^u \Rightarrow \boldsymbol{I}^u = \sqrt{\boldsymbol{I}_a^{u^2} + \boldsymbol{I}_r^{u^2}}. \tag{14}$$

D. Complete Current Decomposition

In conclusion, the phase currents can be split as follows:

$$\underline{i} = \underline{i}_a^b + \underline{i}_r^b + \underline{i}^u + \underline{i}_v. \tag{15a}$$

All terms are orthogonal, thus,

$$\boldsymbol{I} = \sqrt{\boldsymbol{I}_a^{b^2} + \boldsymbol{I}_r^{b^2} + \boldsymbol{I}^{u^2} + \boldsymbol{I}_v^2}. \tag{15b}$$

We emphasize once more that the earlier definitions are valid, and keep their physical meaning, for whichever voltage and current waveform, supply asymmetry and load unbalance.

IV. Power Terms Under Periodic, Nonsinusoidal Operation

From (15b), the apparent power defined by (4a) is decomposed as follows:

$$\boldsymbol{A}^2 = \boldsymbol{U}^2\boldsymbol{I}_a^{b^2} + \boldsymbol{U}^2\boldsymbol{I}_r^{b^2} + \boldsymbol{U}^2\boldsymbol{I}^{u^2} + \boldsymbol{U}^2\boldsymbol{I}_v^2 = P^2 + Q^2 + N^2 + V^2 \tag{16}$$

where $P = \boldsymbol{U}\boldsymbol{I}_a^b$ is *active power*, $Q = \boldsymbol{U}\boldsymbol{I}_r^b$ is *reactive power*, $N = \boldsymbol{U}\boldsymbol{I}^u$ is *unbalance power*, and $V = \boldsymbol{U}\boldsymbol{I}_v$ is *void power*. Note from (11) that the reactive power can be expressed as follows:

$$Q = \frac{\boldsymbol{U}}{\widehat{\boldsymbol{U}}}W = \omega W \frac{\sqrt{1 + (\mathrm{THD}\,(\underline{u}))^2}}{\sqrt{1 + (\mathrm{THD}(\underline{\widehat{u}}))^2}} \tag{17a}$$

where ω is angular line frequency and THD is total harmonic distortion, i.e.,

$$\mathrm{THD}\,(\underline{u}) = \frac{\sqrt{\boldsymbol{U} - \boldsymbol{U}_f}}{\boldsymbol{U}_f} \qquad \mathrm{THD}(\underline{\widehat{u}}) = \frac{\sqrt{\widehat{\boldsymbol{U}} - \widehat{\boldsymbol{U}}_f}}{\widehat{\boldsymbol{U}}_f}. \tag{17b}$$

In (17b) $\boldsymbol{U}_f$ and $\widehat{\boldsymbol{U}}_f$ are the collective rms values of fundamental phase voltages and their unbiased integrals, which are related by $\boldsymbol{U}_f = \omega\widehat{\boldsymbol{U}}_f$.

Equation (17a) shows that, unlike reactive energy *W*, reactive power *Q* is not conservative. In fact, it depends on local voltage distortion.

Note finally that all current and power terms defined earlier can be derived from basic phase quantities, namely, active power P_n, reactive energy W_n, and rms voltage terms U_n and $\widehat{U}_n$.

These quantities are evaluated directly in the time domain and can be measured by simple instrumentation.

Note also that the power terms defined by the CPT are generally different from those considered in traditional metering approaches. However, they provide an insight on relevant physical phenomena, i.e., power consumption and energy storage, which should be taken into account for revenue metering.

V. Accountability

The CPT clarifies the meaning of active, reactive, unbalance and void current, and power terms, and sets the basis for consistent power measurements under asymmetrical and distorted operation. In this section, we approach the accountability problem, i.e., the problem of separating supply and load responsibility on the generation of unbalance and distortion. Consider that, in general, current harmonics can be caused by inherent load nonlinearity and/or by supply voltage distortion. Similarly, asymmetrical currents can be generated by load and/or supply voltage asymmetry.

In general terms, it is very difficult to develop a theory, which is able to separate source and load contributions to distortion and unbalance, when only measurements at the point of power delivery [point of common coupling (PCC)] are available. There are previous papers on the separation of load and source responsibility on distortion [26]–[29], but it was not possible to establish a theoretical background, which is valid in every operating condition.

The CPT and related decompositions offer a viable tool to establish an accountability approach, which gives some meaningful information under practical operating conditions. For this aim, let us assume a three-phase system and measure phase quantities (P_n, W_n, U_n, and $\widehat{U}_n$) at PCC. We then estimate the power terms (i.e., active, reactive, unbalance, and void power), which would be absorbed by the load if it was fed by purely sinusoidal and symmetrical voltages. This portion is accounted to the load, while the rest is accounted to the supply. This simple procedure is based on two assumptions.

1) First, we assume that supply voltage asymmetry and distortion are not caused by the load. This is true only if rated load power is much smaller than grid power capability at PCC.
2) Second, we assume that equivalent phase parameters G_n and B_n keep the same value irrespective of voltage asymmetry and distortion. This corresponds to a very rough approximation of load operation, which can, however, be refined if a more accurate load modeling is available.

The fundamental positive-sequence voltages $\underline{u}_f^p$ at PCC can be computed according to the procedure described in [24], which only requires elementary operations in the time domain. Since such voltages are sinusoidal and symmetrical, their rms value U_f^p is the same in all phases, thus: $\boldsymbol{U}_f^p = \sqrt{3}U_f^p$. Moreover, $\widehat{U}_f^p = U_f^p/\omega$.

According to the aforementioned assumptions, the active power and current terms accountable to the load are as follows:

$$P_{\ell n} = G_n U_f^{p^2} \Rightarrow P_\ell = \sum_{n=1}^{3} P_{\ell n} = U_f^{p^2} \sum_{n=1}^{3} G_n$$

$$I_{a\ell n} = G_n U_f^p \Rightarrow \boldsymbol{I}_{a\ell} = \sqrt{\sum_{n=1}^{3} I_{a\ell n}^2} = U_f^p \sqrt{\sum_{n=1}^{3} G_n^2}. \quad (18a)$$

Similarly, for reactive energy and current, the terms accountable to the load are as follows:

$$W_{\ell n} = B_n \widehat{U}_f^{p^2} \Rightarrow W_\ell = \sum_{n=1}^{3} W_{\ell n} = \widehat{U}_f^{p^2} \sum_{n=1}^{3} B_n = \left(\frac{U_f^p}{\omega}\right)^2 \sum_{n=1}^{3} B_n$$

$$\boldsymbol{I}_{r\ell n} = B_n \widehat{U}_f^p \Rightarrow \boldsymbol{I}_{r\ell} = \sqrt{\sum_{n=1}^{3} I_{r\ell n}^2} = \widehat{U}_f^p \sqrt{\sum_{n=1}^{3} B_n^2} = \frac{U_f^p}{\omega} \sqrt{\sum_{n=1}^{3} B_n^2}. \quad (18b)$$

From (18), we derive parameters G_ℓ^b and B_ℓ^b of the equivalent balanced load and the corresponding balanced active and reactive currents

$$G_\ell^b = \frac{P_\ell}{3U_f^{p^2}} \qquad \boldsymbol{I}_{a\ell}^b = \frac{P_\ell}{\sqrt{3}U_f^p}$$
$$B_\ell^b = \frac{W_\ell}{3\widehat{U}_f^{p^2}} \qquad \boldsymbol{I}_{r\ell}^b = \frac{W_\ell \omega}{\sqrt{3}U_f^p}. \quad (19)$$

From (12b) and (13b), we can then compute the collective rms values of the active and reactive unbalance currents. Given the current components, we immediately derive the corresponding power terms according to (16).

Note that also the void power should be revised for accountability, according to the procedure described in [25]. However, this is needed only in those situations, not frequent in practice, where the void power has a considerable amount compared to other power terms. In all other cases, we assume $\boldsymbol{I}_{v\ell} \approx \boldsymbol{I}_v$.

VI. Remote Control of Distributed Compensators

The CPT sets also a basis for remote control of every type of compensator, i.e., switching power compensators (SPC) and static VAR compensators (SVC). SVC include low-frequency compensators, like thyristor-switched capacitors (TSC) , thyristor-controlled reactors (TCR), and static compensator (STATCOM). SPC include high-frequency compensators, like active power filters (APF) and switching power interfaces (SPI), connected between energy sources and grid. The compensation capabilities are different, since TSC are mostly used for reactive compensation, while TCR allow reactive and unbalance compensation [23]. STATCOM allow all types of low-frequency compensation, while SPC operate in the multikilohertz range and provide harmonic mitigation too [13], [21], [35].

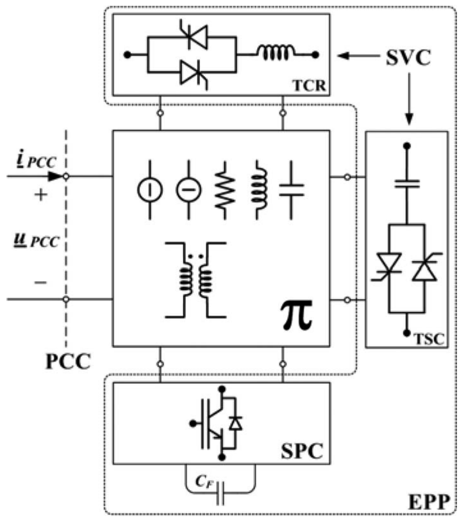

Fig. 1. Microgrid with distributed compensators.

In this section, we discuss the control methods applicable to the various compensators under the assumption that they are driven by conservative power and energy commands [16]. The use of control commands based on conservative quantities allows them to be partitioned and addressed to a variety of remote compensators, with the intent to take full advantage of the compensation capability distributed over the network.

Fig. 1 gives a microgrid representation, where distributed compensators are shown separately, while the other networks components (distribution lines, transformers, loads, energy sources, etc.) are included in box π. In this section, we separately analyze the control techniques applicable to SVC and SPC [20].

A. Control of TSC

Each phase of a TSC is made up of a set of parallel branches, each one including a capacitor in series with thyristor switch. By switching ON and OFF the various branches, the total capacitance can be varied stepwise in the range $0 \leq C \leq C_{\max}$. Usually TSC operation is symmetrical and all phases show the same capacitance *C*. Assuming a three-phase TSC with delta-connected capacitors, according to (3c), the total reactive energy absorbed by the compensator is as follows:

$$W^{\rm TSC} = -C\left(U_{12}^2 + U_{23}^2 + U_{31}^2\right) \tag{20}$$

where U_{12}, U_{23}, and U_{31} are the rms line-to-line voltages. When the TSC receives a reactive energy command, its controller determines the needed capacitance from (20).

B. Control of TCR

A three-phase TCR is made up of three delta-connected branches, each including an inductor $L_{\max}$ and a thyristor switch. By phase-controlling the thyristors, the equivalent phase inductances are continuously regulated in the range $0 \leq L \leq L_{\max}$. The TCR can, therefore, be represented by three controllable reactivities $B_{12},\ B_{23},$ and B_{31}. According to (3b), the total reactive energy taken by the TCR is as follows:

$$W^{\rm TCR} = B_{12}\widehat{U}_{12}^{\,2} + B_{23}\widehat{U}_{23}^{\,2} + B_{31}\widehat{U}_{31}^{\,2}. \tag{21}$$

If the TCR is required to provide reactive energy compensation only, the three reactivities are set equal and their value is determined from (21) based on line-to-line voltage measurement.

A more complex situation occurs if the TCR performs unbalance compensation too. In fact, the unbalance power defined by (16) is not conservative, and is therefore not suitable for remote control of TCR. A solution can be found by making reference to the sequence components defined in [24]. Consider, in fact, that unbalance is considerably attenuated if the TCR compensates for negative-sequence currents absorbed by the load, and this can be achieved by a suitable choice of parameters $B_{12},\ B_{23},$ and B_{31}. The problem is greatly simplified by considering only the fundamental positive-sequence component of the supply voltages ($\underline{u}_f^p$). In fact, the other voltage components are useless for reactive power and unbalance compensation and can be neglected for TCR control purposes. With this assumption, the negative-sequence currents absorbed by the TCR become

$$\underline{i}_f^n = -\begin{vmatrix} B_{23} & B_{12} & B_{31} \\ B_{12} & B_{31} & B_{23} \\ B_{31} & B_{23} & B_{12} \end{vmatrix} \cdot \widehat{\underline{u}}_f^{\,p}. \tag{22}$$

Observing that currents $\underline{i}_f^n$ do not change by adding a common quantity to all rectivities, we can arbitrarily assume $B_{31} = 0$. Let U_f^p and I_f^n be the rms values of voltages $\underline{u}_f^p$ and currents $\underline{i}_f^n$, respectively, the fundamental unbalance power is defined as follows:

$$N_f = 3U_f^p I_f^n. \tag{23a}$$

From easy computations, we derive the relation between N_f and parameters B_{12} and B_{23}

$$\begin{cases} N_f \cos\varphi^n = -\sqrt{3}\dfrac{U_f^{p^2}}{2\omega}B_{12} \\ N_f \sin\varphi^n = \dfrac{U_f^{p^2}}{2\omega}\left(2B_{23} - B_{12}\right) \end{cases} \tag{23b}$$

where φ_n is the phase displacement between voltage u_{f1}^p and current i_{f1}^n. It is worth noting that unbalance power terms $N_f \cos\varphi^n$ and $N_f \sin\varphi^n$ are conservative, thus they can be used for remote control of SVC. The unbalance power command can be expressed in complex terms as follows:

$$\dot{N}_f = N_f \cos\varphi^n + jN_f \sin\varphi^n. \tag{23c}$$

When the TCR receives an unbalance power command, its controller determines the values of B_{12} and B_{23} from (23b). If they are both positive, the solution is acceptable. Otherwise, a common quantity is added to $B_{12},\ B_{23},$ and B_{31} to make two of them positive and the third zero.

It can be demonstrated that unbalance compensation limits the reactive power compensation capability of the TCR by an amount up to $3N_f$.

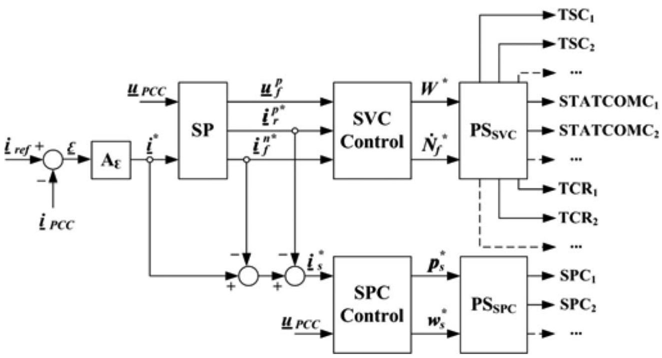

Fig. 2. Concept scheme of cooperative control for distributed compensators.

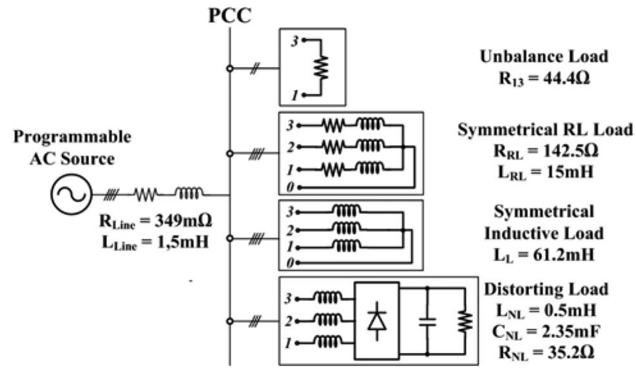

Fig. 3. Experimental three-phase four-wire circuit.

C. Control of SPC

SPC are capable of high-frequency operation, i.e., they can compensate for every power or current term (reactive, unbalance, and void) also in presence of asymmetrical and distorted supply [19]. For this purpose, they are driven by instantaneous power and energy commands (p^{SPC} and w^{SPC}). In three-phase SPC, these commands are transformed into current commands $\underline{i}^{\mathrm{SPC}}$, considering that

$$\begin{cases} \underline{u}\circ \underline{i}^{\mathrm{SPC}} = p^{\mathrm{SPC}} \\ \hat{\underline{u}}\circ\underline{i}^{\mathrm{SPC}}=w^{\mathrm{SPC}} \\ \sum_{n=1}^{3} i_n^{\mathrm{SPC}}=0\end{cases} \Rightarrow \underline{i}^{\mathrm{SPC}} = \begin{vmatrix} u_1 & u_2 & u_3\\ \hat{u}_1 & \hat{u}_2 & \hat{u}_3 \\ 1&1&1\end{vmatrix}^{-1} \begin{vmatrix} p^{\mathrm{SPC}}\\ w^{\mathrm{SPC}}\\0\end{vmatrix}. \tag{24}$$

Current commands $\underline{i}^{\mathrm{SPC}}$ are then executed according to usual current control techniques.

VII. Cooperative Control Principle

The implementation of cooperative control is widely discussed in literature [14]–[19], [32]–[34]. Here, we do summarize the principle of operation based on the application of CPT [20]. The concept control scheme for distributed compensators is shown in Fig. 2. It refers to a situation, where control aims at improving the power factor at PCC by properly driving all available compensators. The controller performs as follows.

1) First of all, the balanced active currents absorbed at PCC are determined, according to (10), and taken as references ($\underline{i}^{\mathrm{ref}}$). In fact, all remaining current terms (reactive, unbalance, and void) should be suppressed by the compensation system.
2) References $\underline{i}^{\mathrm{ref}}$ are then compared with actual currents absorbed at PCC ($\underline{i}^{\mathrm{PCC}}$) to generate error signals $\underline{\varepsilon}$, which are processed by error amplifier A_ε to generate internal current references $\underline{i}^*$.
3) References $\underline{i}^*$, together with PCC voltages $\underline{u}^{\mathrm{PCC}}$, are then fed to sequence processor SP to extract fundamental positive-sequence voltages $\underline{u}_f^p$ and reference currents $\underline{i}_r^{p*}$(fundamental positive-sequence reactive currents) and $\underline{i}_f^{n*}$(fundamental negative-sequence currents), to be compensated by the SVC system.
4) The references for the SPC system are determined by difference as: $\underline{i}_s^* = \underline{i}^* - \underline{i}_r^{p*} - \underline{i}_f^{n*}$.

TABLE I
Fundamental Voltages for Cases I and II

Case I	Case II
$U_1 = 127\angle 0^{\circ}$ VRMS	$U_1 = 127\angle 0^{\circ}$ VRMS
$U_2 = 127\angle{-120}^{\circ}$ VRMS	$U_2 = 113\angle 255{,}6^{\circ}$ VRMS
$U_3 = 127\angle 120^{\circ}$ Vrms	$U_3 = 135\angle 144^{\circ}$ Vrms

5) The SVC control generates total reactive power command W^* and unbalance power command $\dot{N}_f^*$ for the SVC system. These commands are then distributed by power sharing unit $\mathrm{PS}_{\mathrm{SVC}}$ among the various SVC according to their type, compensation capability, and distance from PCC.
6) Similarly, the SPC control unit generates instantaneous active power and reactive energy commands p_s^* and w_s^* for the SVC system. These commands are then distributed by power sharing unit $\mathrm{PS}_{\mathrm{SPC}}$ among the various SPC, according to their compensation capability and distance from PCC.

VIII. Application Examples

A. Example 1—Revenue Metering

In order to analyze the proposed accountability approach, a general purpose virtual instrument has been implemented, based on dual-core PC and eight-channel acquisition board (DAQmx PCI-6143-S, by National Instruments, Austin, TX). The analog signals are measured by means of Hall-effect voltage and current transducers (LV-25P and LA-55P, by LEM). The acquisition routines are implemented by means of a graphical programming language (LabView), while CPT calculations are implemented in C++ and compiled into dynamic link libraries accessed by LabView.

Fig. 3 shows the experimental setup, including programmable ac voltage source, line impedance, linear, and nonlinear loads. The measures are done at PCC. The selected line impedance causes a voltage drop around 10% for rated load, corresponding to a weak power grid, e.g., a smart microgrid. Four different supply situations have been considered.

1) Case I—Symmetrical sinusoidal voltages.
2) Case II—Asymmetrical sinusoidal voltages.
3) Case III—Symmetrical nonsinusoidal voltages.
4) Case IV—Asymmetrical nonsinusoidal voltages.

TABLE II
POWER TERMS MEASURED AT PCC AND ACCOUNTED TO THE LOAD FOR THE CIRCUIT OF FIG. 3

	Case I		Case II		Case III		Case IV	
	PCC	LOAD	PCC	LOAD	PCC	LOAD	PCC	LOAD
Apparent Power	4547,95	4533,14	5869,95	5537,18	4522,01	4459,69	5793,25	5410,45
Active Power	3704,11	3683,46	4091,37	3666,71	3616,05	3550,39	4024,69	3558,61
Reactive Power	2311,04	2316,83	2518,05	2476,9	2380,73	2369,71	2508,8	2452,04
Unbalance Power	791,83	788,36	2586,66	2564,63	792,85	782,41	2524,83	2480,07
Void Power	998,31	996,16	2165,43	2122,07	1038,04	1027,54	2167,22	2108,56

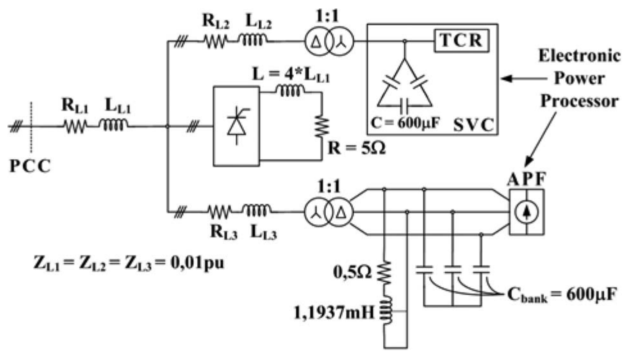

Fig. 4. Simulated network.

Table I shows the rms value and phase of fundamental voltages applied in cases I and II. The phase voltages for cases III and IV have the same fundamental component of cases I and II, with the addition of third, fifth, seventh, and ninth harmonics (the amplitude of each harmonic is 5% of fundamental component).

The accountability approach of Section V was applied, and Table II shows the results of power measurements at PCC and the corresponding power terms accounted to the load.

1) *Case I:* In spite of the sinusoidal and symmetrical voltage supply, the power terms accounted to the load are slightly different from the measured ones. This is the effect of the voltage drops across line impedances, which reflect the asymmetry and distortion of load currents and affect the voltages at PCC. Also, the computation of parameters G_n and B_n is influenced by these voltage drops, thus contributing to the differences between power terms. In practice, since the THD of PCC voltages is less than 6%, the power terms accounted to the load are very close to the measured quantities.
2) *Case II:* The power terms measured to the PCC and accounted to the load are now different, especially the active power, which differs about 10%. This is the effect of asymmetrical supply voltages and voltage drops on line impedances, which cause asymmetry and distortion of the voltages at PCC (phase voltages distortion is 9.7%, 5%, and 8.5%, respectively).
3) *Case III:* In this case, the THD of phase voltages is about 13%, while asymmetry is negligible (less than 1%). Since terms G_n and B_n are moderately influenced by voltage distortion, the power terms accounted to the load are slightly different (less than 2%) from the measured ones.
4) *Case IV:* This is the worst case, where phase voltages are asymmetrical and distorted. The apparent and active power accounted to the load are significantly lower than those measured at PCC, due to the depuration of the effects of voltage asymmetry and distortion. In particular, the active power accounted to the load is 12% lower than that measured at PCC.

B. *Example 2—Cooperative Control*

As an example of application of cooperative control, the network of Fig. 4 was simulated. It includes unbalanced and distorting loads, transmission lines, transformers, and compensation units (fixed capacitor bank, TCR, and APF). The supply voltages fed at PCC are asymmetric and distorted.

The network operation is first analyzed without any type of compensation ($t < 0.2$ s). At $t = 0.2$ s, the SVC is turned ON and compensates for reactive power and load unbalance. At $t = 0.6$ s, also the APF is turned ON and compensates for the remaining unwanted current terms. Finally, at $t = 1.2$ s, a sudden load change is introduced (control angles of thyristor rectifier delayed by 50°) to analyze control dynamics. The control performs according to the principle discussed in the Section VI.

The system operation is described by making reference to the voltage and current waveforms at PCC.

The asymmetry and distortion of supply voltages is appreciable in Fig. 5, while Fig. 6 shows the current waveforms in the initial situation, when all compensators are OFF. The high current distortion is due not only to the thyristor rectifier but also to the capacitor bank, which is supplied by distorted voltages. The current asymmetry is due to load unbalance and voltage asymmetry.

Fig. 7 shows the currents at PCC after turning ON the SVC. Although distorted, the currents are now smaller than before, due to the reduction of reactive and unbalance terms.

Fig. 8 shows the currents at PCC after turning ON the APF too. Within the control bandwidth, the input currents now include balanced active terms only and track the supply voltages with good accuracy.

Finally, Fig. 9 shows the behavior of power factor λ at PCC. Initially, the power factor is very low, due to unbalance, distortion, and reactive power. The intervention of the SVC reduces reactive and unbalance currents, thus the power factor steps up.

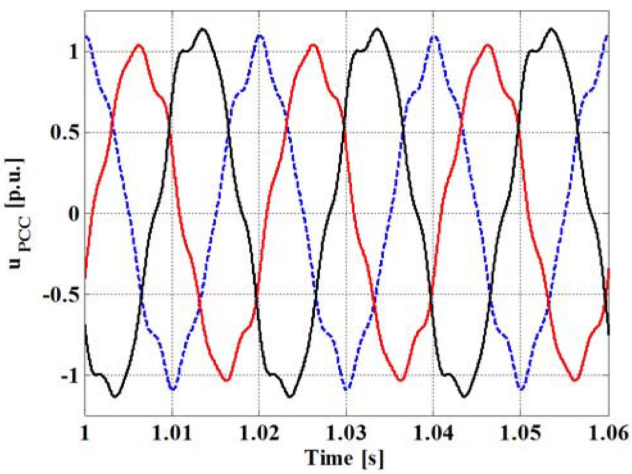

Fig. 5. Line voltages at PCC.

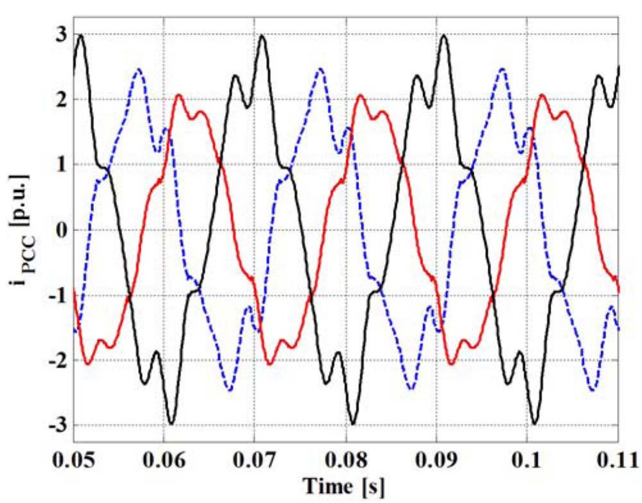

Fig. 6. Line currents at PCC with SVC and APF turned OFF.

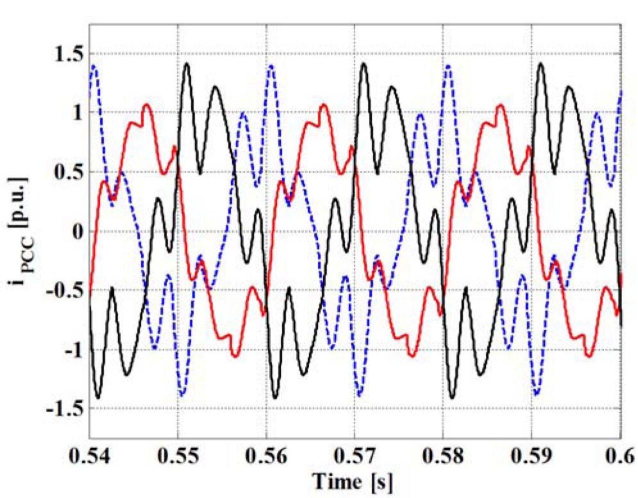

Fig. 7. Line currents at PCC with SVC turned ON.

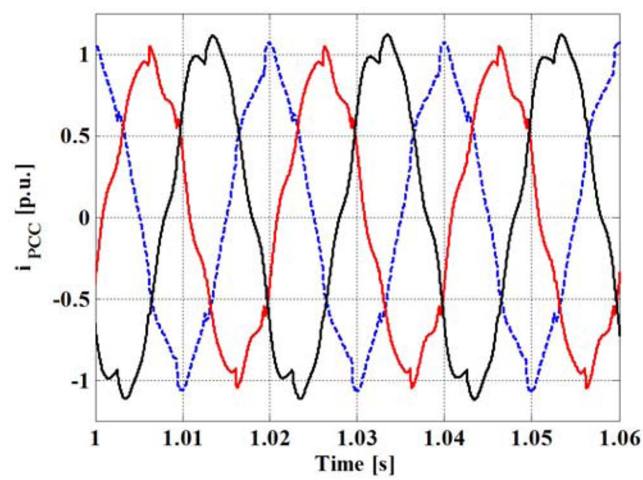

Fig. 8. Currents at PCC with SVC and APF turned ON.

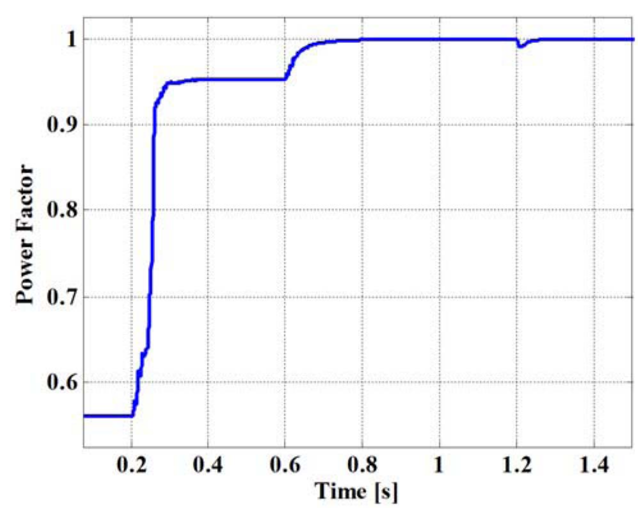

Fig. 9. Time behavior of power factor.

The power factor improves further, approaching unity, after intervention of the APF, which removes every residual reactive and unbalance currents together with void currents, including those generated by the SVC. The effect of the load transient on the power factor is minimal, showing that the system reacts properly to a sudden active and reactive power variation.

IX. Conclusion

The paper shows that CPT provides a platform to approach the problems of power measurement and compensation in smart microgrids, where supply voltage distortion and frequency variation can considerably affect system operation.

Active and reactive current and power terms have been initially revisited to suit conditions, where voltages and currents can be severely distorted. An extension to polyphase circuits has also been discussed to identify the effects of supply asymmetry and load unbalance.

An accountability approach has then been introduced, which provides a criterion to separate load and supply responsibility on the generation of active, reactive, and unbalance power.

The application of CPT to remote control of compensators has also been approached, showing that the theory is applicable to every type of compensator and can be the basis for cooperative control of distributed compensators in microgrids.

The accountability and control approaches have finally been tested experimentally and by simulation, to show their capabilities in a working scenario of practical interest.

Appendix

Periodic Variables and Their Properties

For periodic quantities (period T, frequency $f = 1/T$, and angular frequency $\omega = 2\pi f$), we define the operators as following:

$$\text{Average value}: \quad \bar{x} = \langle x \rangle = \frac{1}{T}\int_0^T x dt \tag{A1a}$$

$$\text{Time derivative:} \quad \breve{x} = \frac{dx}{dt} \tag{A1b}$$

$$\text{Time integral:} \quad x_\int = \int_0^t x(\tau)\, d\tau \tag{A1c}$$

$$\text{Unbiased time integral:} \quad \hat{x} = x_\int - \bar{x}_\int \tag{A1d}$$

$$\text{Internal product:} \quad \langle x, y \rangle = \frac{1}{T}\int_0^T xy dt \tag{A1e}$$

$$\text{Norm (rms value):} \quad X = \|x\| = \sqrt{\langle x, x \rangle} \tag{A1f}$$

$$\text{Orthogonality:} \quad \langle x, y \rangle = 0. \tag{A1g}$$

For vector quantities $\underline{x}$ and $\underline{y}$ of size N, we define

$$\text{Scalar product:} \quad \underline{x} \circ \underline{y} = \sum_{n=1}^{N} x_n y_n \tag{A2a}$$

$$\text{Internal product:} \quad \langle \underline{x}, \underline{y} \rangle = \sum_{n=1}^{N} \langle x_n, y_n \rangle \tag{A2b}$$

$$\text{Norm:} \quad \boldsymbol{X} = \|\underline{x}\| = \sqrt{\sum_{n=1}^{N} \langle x_n, x_n \rangle} = \sqrt{\sum_{n=1}^{N} X_n^2}. \tag{A2c}$$

The vector norm is also called *collective rms* value. The earlier quantities have the following properties:

$$\langle x, \breve{x} \rangle = 0 \quad \langle x, \hat{x} \rangle = 0 \tag{A3a}$$

$$\langle x, \breve{y} \rangle = -\langle \breve{x}, y \rangle \quad \langle x, \hat{y} \rangle = -\langle \hat{x}, y \rangle \tag{A3b}$$

$$\langle x, y \rangle = -\langle \breve{x}, \hat{y} \rangle = -\langle \hat{x}, \breve{y} \rangle. \tag{A3c}$$

Conservative Power and Energy Terms

Considering network Π with L branches, a set of voltages $\{u_\ell\}_{\ell=1}^{L}$ and currents $\{i_\ell\}_{\ell=1}^{L}$ is said to be *consistent* with the network if they satisfy the Kirchoff's Law for voltages (KLV) and currents (KLC), respectively. It is easy to show that if branch voltages u_ℓ are consistent with the network, the same happens for quantities $\breve{u}_\ell$ and $\hat{u}_\ell$. Similarly for branch currents i_ℓ and related quantities $\breve{i}_\ell$ and $\hat{i}_\ell$. According to the Tellegen's theorem, we can therefore affirm that every scalar product of KLV-consistent terms u_ℓ, $\breve{u}_\ell$, and $\hat{u}_\ell$ and KLC-consistent terms i_ℓ, $\breve{i}_\ell$, and $\hat{i}_\ell$ is a conservative quantity.

References

[1] C. I. Budeanu, *Puissances Reactives et Fictives*. Bucharest, Romania: Inst. Romain de l.Energie, 1927.

[2] S. Fryze "Wirk-, Blind-, Scheinleistung in Elektrische Stromkreisen mit Nichtsinusformingen Verlauf von Strom und Spannung," *ETZ*, Bd. 53, pp. 596–599, 625–627, 700–702, 1932.

[3] W. Shepherd, P. Zakikhani, "Suggested definition of reactive power for nonsinusoidal systems," in *Proc. Inst. Elec. Eng.*, vol. 119, Sep. 1972, pp. 1361–1362.

[4] L. S. Czarnecki, "Orthogonal decomposition of the currents in a 3-phase nonlinear asymmetrical circuit with a nonsinusoidal voltage source," *IEEE Trans. Instrum. Meas.*, vol. IM-37, no. 1, pp. 30–34, Mar. 1988.

[5] P. Tenti and P. Mattavelli, "A time-domain approach to power term definitions under non-sinusoidal conditions," *L'Energia Elettrica*, vol. 81, pp. 75–84, 2004.

[6] L. S. Czarnecki, "Currents' physical components (CPC) in circuits with nonsinusoidal voltages and currents. Part 1: Single-phase linear circuits," *Electr. Power Qual. Utilizat. J.*, vol. XI, no. 2, pp. 3–14, 2005.

[7] J. L. Willems, "Power factor correction for distorted bus voltages," *Electr. Mach. Power Syst.*, vol. 13, no. 4, pp. 207–218, 1987.

[8] L. S. Czarnecki, "Power factor improvement of three-phase unbalanced loads with nonsinusoidal supply voltages," *ETEP Eur. Trans. Electr. Power Eng.*, vol. 3, no. 1, pp. 67–72, Jan./Feb. 1993.

[9] H. Akagi, Y. Kanazawa, and A. Nabae, "Generalized theory of the instantaneous reactive power in three-phase circuits," in *Proc. Int. Power Electr. Conf.*, Tokyo/Japan, 1983, pp. 1375–1386.

[10] H. Akagi, Y. Kanazawa, and A. Nabae, "Instantaneous reactive power compensators comprising switching devices without energy storage components," *IEEE Trans. Ind. Appl.*, vol. IA-20, no. 3, pp. 625–630, May/Jun. 1984.

[11] M. Depenbrock, "The FBD-method, A generally applicable tool for analyzing power relations," *IEEE Trans. Power Syst.*, vol. 8, no. 2, pp. 381–387, May 1993.

[12] L. Cristaldi and A. Ferrero, "Mathematical foundations of the instantaneous power concept: An algebraic approach," *ETEP Eur. Trans. Electr. Power*, vol. 6, no. 5, pp. 305–309, Sep./Oct. 1996.

[13] H. Akagi, H. Fujita, and K. Wada, "A shunt active filter based on voltage detection for harmonic termination of a radial power distribution line," *IEEE Trans. Ind. Appl.*, vol. 35, no. 3, pp. 638–645, May/Jun. 1999.

[14] P. Jintakosonwit, H. Fujita, H. Akagi, and S. Ogasawara, "Implementation and performance of cooperative control of shunt active filters for harmonic damping throughout a power distribution system," *IEEE Trans. Ind. Appl.*, vol. 39, no. 2, pp. 556–563, Mar./Apr. 2003.

[15] P. T. Cheng and T. L. Lee, "Analysis of harmonic damping effect of the distributed active filter system," *IEEE Trans. Ind. Appl.*, vol. 126, no. 5, pp. 605–614, May 2006.

[16] P. Tenti, E. Tedeschi, and P. Mattavelli, "Compensation techniques based on reactive power conservation," *Electr. Power Qual. Utilizat.*, vol. XIII, no. 1, pp. 17–24, 2007.

[17] P. T. Cheng and T. L. Lee, "Distributed active filter systems (DAFS): A new approach to power systems harmonics," *IEEE Trans. Ind. Appl.*, vol. 42, no. 5, pp. 1301–1309, Sep./Oct. 2006.

[18] P. T. Cheng, T. L. Lee, H. Akagi, and H. Fujita, "A dynamic tuning method for distributed active filter systems," in *Proc. IEEE IAS 41st Annu. Meeting*, 2006, pp. 175–182.

[19] E. Tedeschi, P. Tenti, and P. Mattavelli, "Cooperative operation of active power filters by instantaneous complex power control," in *Proc. 7th Int. Conf. Power Electron. Drive Syst.*, Bangkok, Nov. 2007.

[20] E. Tedeschi, P. Tenti, P. Mattavelli, and D. Trombetti, "Cooperative control of electronic power processors in micro-grids," *Braz. J. Power Electron.*, vol. 14, pp. 241–249, Nov. 2009.

[21] E. H. Watanabe, J. L. Alfonso, J. G. Pinto, L. F. C. Monteiro, M. Aredes, and H. Akagi, "Instantaneous p-q power theory for control of

compensators in micro-grids," *Prz. Elektrotech. (Electr. Rev.)*, vol. 86, no. 6, pp. 1–10, 2010.

[22] A. Monti, F. Ponci, A. Benigni, and J. Liu, "Distributed intelligence for smart grid control," *Prz. Elektrotech. (Electr. Rev.)*, vol. 86, no. 6, pp. 38–47, 2010.

[23] L. Gyugyi, R. A. Otto, and T. H. Putman, "Principles and applications of static, thyristor-controlled, shunt compensators," *IEEE Trans. Power App. Syst.*, vol. PAS-97, no. 5, pp. 1935–1945, Sep./Oct. 1978.

[24] P Tenti, J. L. Willems, P. Mattavelli, and E. Tedeschi, "Generalized symmetrical components for periodic non-sinusoidal three-phase signals," *Electr. Power Qual. Utilizat.*, vol. XIII, no. 1, pp. 9–15, 2007.

[25] P. Tenti, P. Mattavelli, H. K. Morales, and Paredes, "Conservative power theory, sequence components and accountability in smart grids," *Prz. Elektrotech.*, vol. 6, pp. 30–37, 2010.

[26] L. Cristaldi and A. Ferrero, "A digital method for the identification of the source of distortion in electric power systems," *IEEE Trans. Instrum. Meas.*, vol. 44, no. 1, pp. 14–18, Feb. 1994.

[27] C. Li, W. Xu, and T. Tayjasant, "A critical impedance-based method for identifying harmonic sources," *IEEE Trans. Power Del.*, vol. 19, no. 2, pp. 671–678, Apr. 2004.

[28] A. Pavas, V. Staudt, and H. Torres-Sánchez, "Discussion on existing methodologies for the responsibilities assigment problem," in *Proc. Int. School on Nonsinusoidal Currents and Compensation*, Lagow, Poland, Jun. 2008.

[29] A. Pavas, V. Staudt, and H. Torres-Sánchez, "Experimental investigation of existing methodologies for the responsibility assignment problem," in *Proc. IEEE Power Tech.*, Bucharest, Romania, Jun./Jul.2009.

[30] G. Venkataramann and C. Marnay, "A large role for microgrids, "Are microgrids a viable paradigm for electricity supply expansion?" *IEEE Power Energy Mag.*, pp. 78–82, May/Jun. 2008.

[31] C. Marnay, H. Asano, S. Papathanassiou, and G. Strbac, "Policymaking for microgrids: Economic and regulatory issues of microgrid implementation," *IEEE Power Energy Mag.*, pp. 66–77, May/Jun. 2008.

[32] E. Barklund, N. Pogaku, M. Prodanovic, C. Hernandez-Aramburo, and T. C. Green, "Energy management in autonomous microgrid using stability-constrained droop control of inverters," *IEEE Trans. Power Electron.*, vol. 23, no. 5, pp. 2346–2352, Sep. 2008.

[33] Y. A.-R. I. Mohamed and E. F. El-Saadany, "Adaptive decentralized droop controller to preserve power sharing stability of paralleled inverters in distributed generation microgrids," *IEEE Trans. Power Electron.*, vol. 23, no. 6, pp. 2806–2816, Nov. 2008.

[34] Y. W. Li and C.-N. Kao, "An accurate power control strategy for power-electronics-interfaced distributed generation units operating in a low-voltage multibus microgrid," *IEEE Trans. Power Electron.*, vol. 24, no. 12, pp. 2977–2988, Dec. 2009.

[35] Y. W. Li, D. M. Vilathgamuwa, and P. C. Loh, "A grid-interfacing power quality compensator for three-phase three-wire microgrid applications," *IEEE Trans. Power Electron.*, vol. 21, no. 4, pp. 1021–1031, Jul. 2006.

Paolo Tenti (F'99) graduated with honors in electrical engineering from the University of Padova, Padova, Italy, in 1975.

He is currently a Professor of electronics in the Department of Information Engineering, University of Padova, Padova, Italy. His research interests include industrial and power electronics, electromagnetic compatibility (EMC), application of modern control methods to power electronics, EMC analysis of electronic equipment, and cooperative control of distributed electronic power processors in smart grids.

Prof. Tenti was a member of the Executive Board of the IEEE Industry Applications Society and a Chair of various society committees from 1991 to 2000. In 1997, he served as the IEEE Industry Applications Society (IAS) President.

In 2000, he was a Chair of the IEEE World Conference on Industrial Applications of Electrical Energy, Rome. During 2000–2001, he was appointed the IEEE IAS Distinguished Lecturer on EMC in industrial equipment.

From 2002 to 2008, he served as the Department Director with the University of Padova and a Chairman of the Board of Directors. He is also President of CREIVen, an industrial consortium for research in industrial electronics with special emphasis on EMC.

Helmo Kelis Morales Paredes (S'09) was born in Puno-Perú, Peru. He received the B.S. degree in electrical engineering from Arequipa National University, Arequipa, Perú, in 2002, and the M.Sc. degree in electrical engineering in 2006 from the University of Campinas (UNICAMP), Campinas, São Paulo, Brazil, where he is currently working toward the Ph.D. degree. From October 2009 to June 2010, he was a Visitor Student in the Department of Information Engineering, University of Padova, Padova, Italy, where he was engaged on Conservative Power Theory and their application to smart microgird.

His current research interests include power quality evaluation and power definitions under nonsinusoidal and/or asymmetries conditions and its application in power conditioning and revenue metering.

Mr. Morales Paredes is a Student Member of the Brazilian Power Electronics Society.

Paolo Mattavelli (M'00) received the Ph.D. degree in electrical engineering in 1995 from the University of Padova, Padova, Italy, in 1995.

From 1995 to 2001, he was a Researcher at the University of Padova. In 2001, he joined as an Associate Professor at the University of Udine, Udine, Italy, where he was leading the Power Electronics Laboratory. In 2005, he joined the University of Padova, Vicenza with the same duties. In 2010, he joined the Bradley Department of Electrical and Computer Engineering at Virginia Tech, Blacksburg, VA as a Professor, where he is currently a member of the Center of Power Electronics Systems.

His research interests include analysis, modeling and control of power converters, digital control techniques for power electronic circuits, and grid-connected converters for power quality and renewable energy systems. In these research fields, he was leading several industrial and government projects.

Prof. Mattavelli is currently an Associate Editor for IEEE Transactions on Power Electronics, and as an Industrial Power Converter Committee Technical Review Chair for the IEEE Transactions on Industry Applications. During 2003–2006 and 2006–2009, he was a member-at-large of the IEEE Power Electronics Society's Administrative Committee. He was also the recipient of the Prize Paper Award in the IEEE Transactions on Power Electronics and in 2007, a second place in the Prize Paper Award at the IEEE Industry Application Annual Meeting.